DESIGN AND FABRICATION OF AN EXPERIMENTAL SET UP FOR AC SUSCEPTIBILITY MEASUREMENT

Thesis Submitted for the Award of the Degree of

Master of Science

By

DEBJANI BANERJEE
409PH2080
Under the academic autonomy

National Institute of Technology, Rourkela

Under the Guidance of

Dr. Prakash Nath Vishwakarma

Department of Physics

National Institute of Technology

Rourkela-769008

2009-2011

CERTIFICATE

This is to certify that the thesis entitled "***design & fabrication of an experimental set up for ac susceptibility measurement***" submitted by Debjani Banerjee in partial fulfilment of the requirements for the award of degree of Master of Science in Physics at National Institute of Technology, Rourkela is an authentic work carried out by her under our supervision. To the best of my knowledge, the matter embodied in this thesis has not been submitted by any other university/ Institute for the award of any degree or diploma.

Date-

Dr. Prakash Nath Vishwakarma
Department of physics
National Institute of Technology
Rourkela-769008

Declaration

I hereby declare that the project work entitled "***design & fabrication of an experimental set up for ac susceptibility measurement"*** Submitted to the NIT,Rourkela, is a record of an original work done by me under the guidance of **Dr. Prakash Nath Vishwakarma** Faculty Member of NIT,Rourkela and this project work has not performed the basis for the award of any Degree or diploma/ associate ship/fellowship and similar project if any.

Date:

DEBJANI BANERJEE
MSc, Physics
NIT, Rourkela

ACKNOWLEDGEMENT

First of all my heartful thanks to almighty for reasons too numerous to mention. My sincere gratitude to my mentor Dr.P.N.Vishwakarma for guiding me all through the course of my project. I truly thank him for his esteemed encouragement from the beginning to the end of the project.

I would also like to acknowledge Achyuta Kumar Biswal and Jashashree Ray for helping a great deal in this work.

I am extremely grateful to my parents for support and blessings.

I heartily thank to my project partner Rakhee Sharma for her co-operation.

In particular, I would thank my friends and Tanmaya Badapanda who by any way stimulated me in the completion of my work.

Dedicated to my parents……...

CONTENTS

Abstract

Chapter-1 Introduction

1.1-introduction

1.2-Magnetic behaviour of a material

1.3-Different methods to measure susceptibility

1.4-Difference between ac and dc susceptibility

1.5-Why ac susceptibility

1.6-Diagram of a typical ac susceptometer

Chapter-2 Design and fabrication

2.1 Cross-Section view of 1st design

2.2 Magnetic field at the centre of the solenoid

2.3 Experimental set up at high temperature**:**

Chapter-3 Sample Preparation

3.1 Sample selection

3.2 Different techniques involved in Preparation

3.3. LSMO Preparation

3.4 Flow chart to prepare LSMO

Chapter- 4 RESULT AND DISCUSSION

4.1. XRD analysis of the LSMO

4.2. Ac Susceptibility of the LSMO

4.3 Conclusion

Chapter 5 Appendix

XRD Analysis of $CoFe_2O_4$

References

ABSTRACT

An Experimental set up for ac susceptibility measurement, is designed and fabricated. The former material chosen is Teflon. The first design consists of a primary coil, a secondary coil and a sample holder. Copper wire (150micron) winding was done on the primary as well as the secondary coil. The secondary coil is a two coil system in which the two winding is in opposite direction to each other. The set-up is based on the phenomenon of "mutual induction". Due to some accident, the first setup got damaged before the experiments could be finished. Hence a second setup is fabricated, but this time the sample holder part is omitted. The sample is directly inserted inside the secondary. To monitor the temperature, a Pt100 sensor is put inside the secondary, in contact with the sample.

To test the setup, $La_{0.67}Sr_{0.33}MnO_3$ (LSMO) is prepared by auto combustion sol gel method. First the LSMO is characterized by XRD and it is found to be single phase. Then the sample is inserted into the sample holder and ac susceptibility is measured, as a function of temperature, higher than 300K.

The measurement is done with the help of a lock in amplifier (SR830) which was computer interfaced. After removing the sample from setup, a empty run is done. The sample data is obtained by subtracting the empty run data from the first run data. Then the graph was plotted between the susceptibility versus temperature. A sharp rise in susceptibility is observed at 90^0C (363K), which is in agreement with the earlier reported values of T_C. Hence, this confirms proper working of our setup.

CHAPTER-1

INTRODUCTION

The history of magnetism is very difficult to dig out, but in the 800 BC, a naturally occurring magnetic material called loadstone was used for navigation purpose. Now a days various magnetic materials in the form of metals, semiconductors, and insulators are known. When a solid is placed in a magnetic field it gets magnetised. Magnetization means the magnetic dipoles inside the material gets aligned along the direction of applied magnetic field. The magnetic moment per unit volume along the direction of magnetic field inside a solid is called magnetisation and is denoted by M. The effect of magnetic field can be expressed as some relation like:

SI	CGS
$B = \mu_0 (H + M)$	$B = H + 4\pi M$
$\frac{B}{H} = \mu_0 \left(1 + \frac{M}{H}\right)$ $\boxed{\Rightarrow \mu = \mu_0 (1 + \chi)}$	$\frac{B}{H} = 1 + \frac{4\pi M}{H}$ $\boxed{\Rightarrow \mu = 1 + 4\pi\chi}$

Where 'B' is magnetic flux density or magnetic induction and is the measure of magnetic lines of force passing per unit area, H is the applied magnetic field and M is the magnetization. μ = B/H is the magnetic permeability and χ = M/H is the susceptibility.

Susceptibility is a measure of the quality of the magnetic material and is defined as the magnetisation produced per unit applied magnetic field. For isotropic medium χ is a scalar quantity. Generally it is a dimensionless quantity. Susceptibility can be quantified in terms of molar/gram/volume susceptibility depending if the measured susceptibility is per unit mole/gram/volume. Experimentally one obtains volume susceptibility. The magnitude and

sign of susceptibility vary with the type of magnetism, and hence characterises the various magnetic materials. Although B, H, and M must necessarily have the same units, it is customarily to denote in CGS (SI) units, 'B' in gauss (tesla, T), 'H' in Oersted, Oe (A/m) and 'M' in erg/Oe cm^3 or emu/cm^3 (A/m).

Now in our project our job is to design of an ac susceptometer and to measure volume susceptibility by this experimental set-up. The dc-magnetometer and the ac susceptometer are two different tools which provide different ways of getting magnetic properties. But both these two techniques depends on sensing coils and is used to measure the variation of the magnetic flux due to magnetic sample.

1.2 Magnetic behaviour of a material:

When a material is placed in a magnetic field then it is magnetized. Both spin motion and orbital motion contribute to it. The major contribution is due to the spin motion of the unpaired valance electrons as well as spin of the nuclei. The motion of electron is nearly equivalent to an electric current which produces the magnetic effects. According to the electronic magnetic moments, a number of magnetic moments may align themselves in different directions to generate a net non-zero magnetic moment. So the nature of magnetization produced depends on the number of unpaired valence electrons present in the atoms of the solid and on the relative orientations of the neighbouring magnetic moments. The magnetism in solids is generally classified into the following five categories:

1.Diamagnetism

2. Paramagnetism

3. Ferromagnetism

4. Antiferromagnetism

5. Ferrimagnetism

Though the magnetic material can be classified according to the nature of the magnetism present. It may however be noted that above a certain critical temperature all material becomes paramagnet.

Diamagnetism is a very weak effect. Diamagnet does not contain any permanent magnetic moments. The existence of a small non-zero magnetic moment in diamagnet is attributed to magnetic field. Example, He, Ne, Ar, Xe, superconductors, etc the orbital motion of the electrons. Here the magnetic moments align opposite to the applied magnetic field.

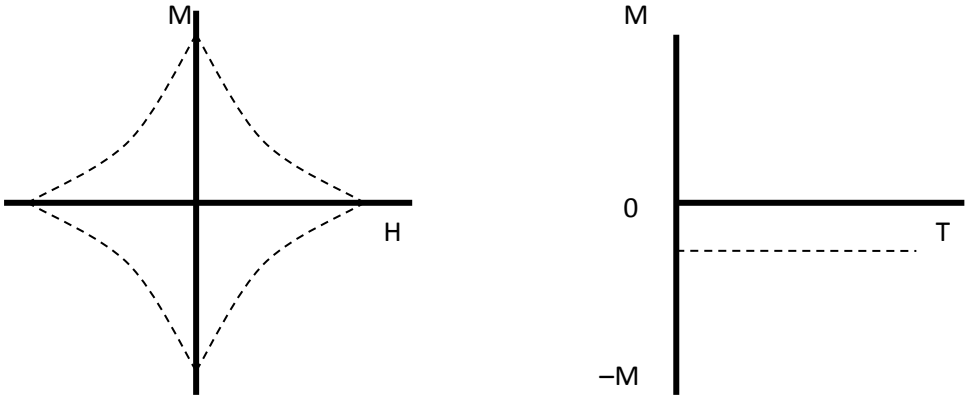

Fig no-1.1 Diamagnetic behaviour of a material (superconductor) [1]

Paramagnetism arises due to the presence of permanent electronic magnetic moment. Para magnetism is also a weak effect but in this case, the magnetic moment alignment is in the direction of the field. Example- Pt, Na

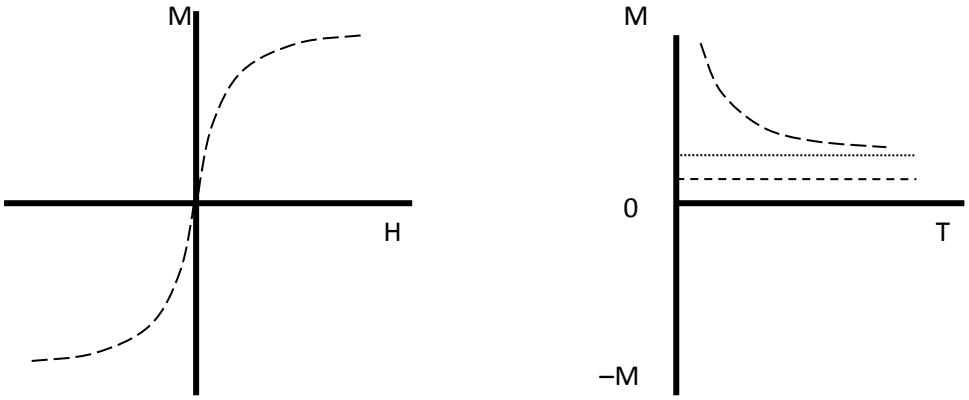

Fig no-1.2 Paramagnetic behaviour of a material [1]. The three lines (top to down) in M-T plot corresponds to Langevin, Van-vleck and Pauli paramagnetism.

Ferromagnetism is a very strong magnetic effect. It arises when the adjacent magnetic moment align themselves in the same direction. It contains domains and has non-zero magnetization even in the absence of magnetic field.

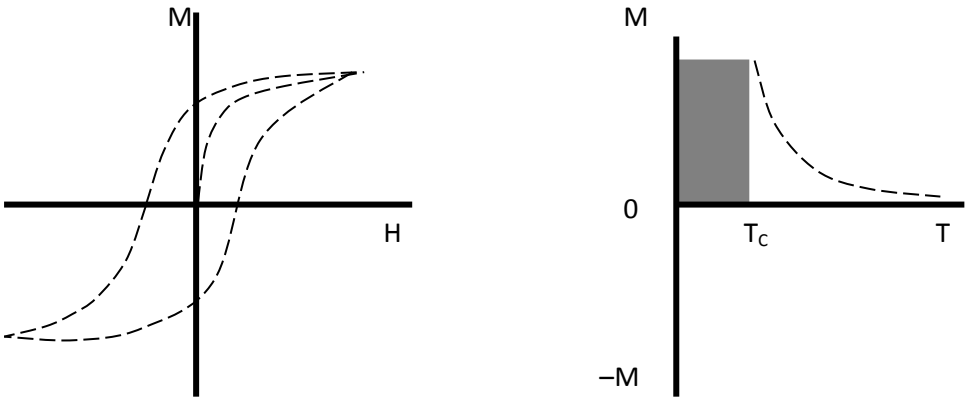

Fig no1.3 Ferromagnetic behaviour of a material [1]

In antiferromagnetism the alignment of adjacent moments are equal and opposite to each other. Complete cancellation of moments take place for a perfect antiferromagnet. E.g., MnO.

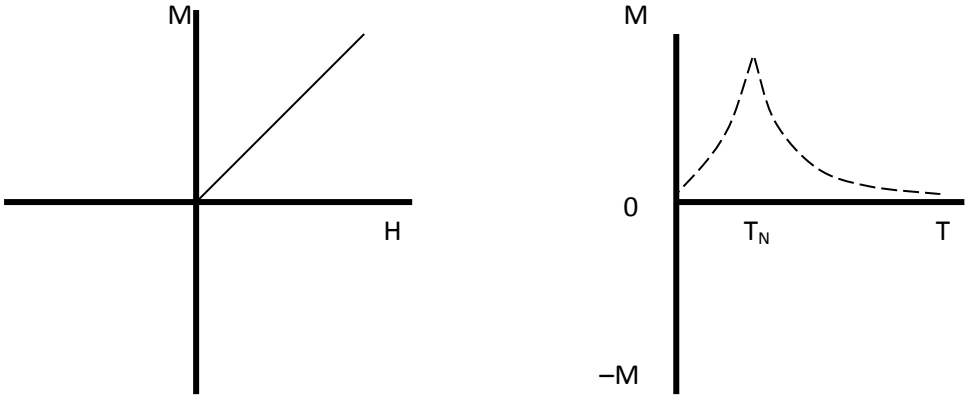

Fig no1.4 Antiferromagnetic behaviour of a material [1]

Ferrimagnetism is similar to antiferromagnet. But in Ferrimagnet that adjacent moments are unequal in magnitude. Hence complete cancellation of moment does not takes place.

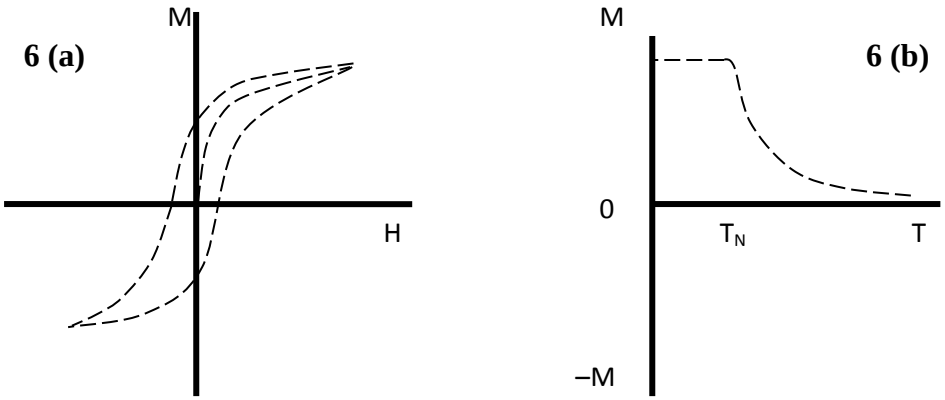

Fig no1.5 Ferrimagnetic behaviour of a material [1]

1.3 Different methods to measure susceptibility:

Vibrating sample method:

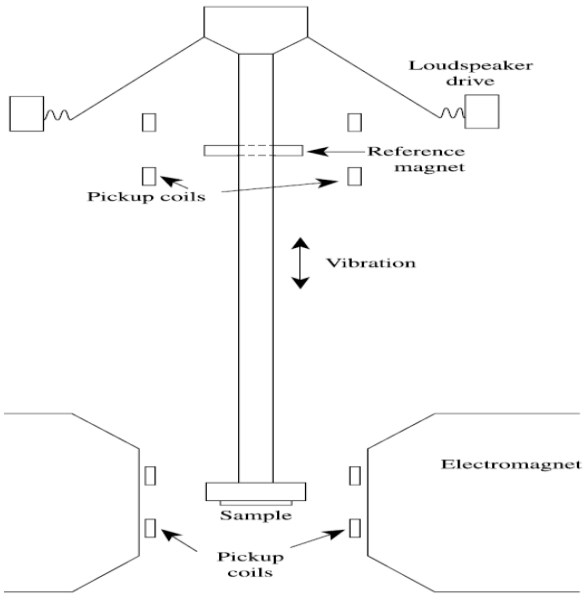

Fig 1.6 Experimental set up of VSM [2]

This method was invented by the scientist Foner[2]. The basic principle is the changing of flux in a coil. A sample is vibrated near the coil. The shape of the sample is usually spherical or small disc, is connected to the end of a rod. The other end of the rod is fixed to a mechanical vibrator. A magnetic field is given, to induced some magnetization in the sample. The voltages we get from the two sides of coils are compared. This difference is proportional to the magnetic moment of the Sample. This method is very versatile and sensitive. And it can be applicable for both weak and strong magnetic substances.

Magnetometer method:

This method is virtually obsolete today. Actually it is very old method and simplest also. The basic principle behind this is a static measurement of the external field of the specimen by means of the deflection produced by the field in the angular position of a suspended magnet. The field applied to the specimen is supplied by a solenoid. In this method the deflection of the magnet measures the magnetization of the entire specimen averaged its volume. Here the shape of the specimen is ellipsoidal. This method is also very sensitive. This sensitivity makes the measurement very difficult that's why it is used very rarely now a day[2]

Ballistic Method:

This is an ac method to measure susceptibility. Here a search coil is wound on the centre of the specimen, which in turn is placed in the centre of a solenoid in the air gape of an electromagnet. The search coil and the solenoid are connected to the flux meter and magnetizing circuits, respectively. If the applied field is H_a and the demagnetization field is H_d then the true field is

$H= Ha-H_d = H_a-N_dM$

This value of H applies only to the centre of the specimen. Applying the value of the magnetic induction B we get,

$H=H_a- (B-H_a)/(4\pi/n_d)-1$

Here N_d=Ballistic demagnetization factor

This method is well studied for rod specimen, particularly when the effect of tension or torsion is studied. This method is quite better.[2]

1.4 DIFFERENCE BETWEEN AC AND DC SUSCEPTIBILITY:

In a dc magnetization measurement a value for the magnetic moment 'M' is measured for some applied dc field, H_{dc}. If the sample being measured does not have a permanent magnetic moment, an applied field is required to magnetize the sample. Usually the moment is measured, as a function of field, and the materials magnetization curve (that is, M versus H_{dc}) is determined. A detection coil is used to detect the change in magnetic flux due to the presence of the magnetic moment. Since the applied magnetic field is constant, there will be no emf induced due to H_{dc} (Faraday's law). The induce emf is generated in the detection coil by moving the sample.

The dc or static susceptibility is thus given by:

$$\chi_{dc} = M / H_{dc}$$

Similar to dc magnetometer, an ac susceptometer uses a detection coil to detect changes in the magnetic flux due to the sample. The main difference lies in how the flux variation is achieved.

On the other hand, in an ac susceptometer the sample is generally centred within a detection coil and magnetized by an ac magnetic field H_{ac}. The magnetic moment of the sample follows the applied field either in-phase or with some phase lag. The detection circuitry is generally balanced with a second identical, but oppositely wound, empty coil to null out the flux changes other that that of sample. As a result, any experimentally detected change in flux is only due to the changing moment of the sample (dM) as it responds to the ac field (no sample movement is required to produce an output signal) and not to the moment itself as in dc technique. The ac susceptibility is:

$$\chi_{ac} = dm / VH_{ac} \rightarrow dM/dH$$

Thus, the ac susceptibility is actually the slope (dM/dH) of the magnetization curve (M versus H curve). The ac technique detects changes in the magnetization that lead to dM/dH in

the limit of small ac fields, and this is why sometimes referred to as a differential susceptibility. This is the fundamental difference between the ac and dc measurement techniques.

In the dc measurement, the magnetic moment of the sample does not change with time. Thus, a static magnetic measurement is performed. An ac output signal is detected in a VSM, but this signal arises from the periodic movement of the sample. In the ac measurement, the moment of the sample is actually changing in response to an applied ac field, allowing the dynamics of the magnetic system to be studied.

Since the actual response of the sample to an applied ac field is measured, the magneto-dynamics can be studied through the complex susceptibility ($\chi'+i\chi''$). The component χ' represents the component of the susceptibility that is in phase with the applied ac field, while χ'' represent the component that is out of phase. The out of phase component χ'' is related to the energy losses, or in other words, the energy absorbed by the sample from the ac field.

1.5 WHY AC SUSCEPTIBILITY?

In case of ac susceptibility:

It has a great application in different fields, like spin glass, superparamagnetism, superconductivity etc. A brief discussion is given below.

SPIN-GLASS

In a spin-glass, magnetic spins experience random interactions with other magnetic spins, resulting in a state that is highly irreversible and metastable. This spin-glass state is realized below the freezing temperature when the relaxation dynamics of spins are too slow. Spin-glass behaviour is usually better characterized by ac susceptibility. The most studied spin-glass systems are dilute alloys of paramagnets or ferromagnets in nonmagnetic metals. The freezing temperature is determined by measuring χ' vs. temperature where a cusp appears at the freezing temperature. Furthermore, the location of the cusp is dependent on the frequency of the AC susceptibility measurement, a feature that is not present in other magnetic systems and therefore confirms the spin-glass phase. Though other techniques have come up to

witness spin glass, ac technique still remains the most authentic measurement for spin-glasses [3].

SUPERPARAMAGNETISM

AC susceptibility measurements are an important tool in the characterization of small ferromagnetic particles. Superparamagnetism, the theory of which was originally explained by Neel and Brown. In this theory, the particles exhibit single-domain ferromagnetic behaviour below the blocking temperature, T_B , and are superparamagnetic above T_B [4].

MAGNETIC PHASE TRANSITIONS

The low frequency susceptibility measurement behaviour is similar to that of dc measurement. Hence low frequency measurement can also reveal the magnetic state as well as magnetic phase transitions (if present).

SUPERCONDUCTIVITY

AC susceptibility is the standard tool for determining the physics of superconductors, in particular for studying magnetic field effect on the superconductor. This is because dc magnetic field cannot penetrate through the superconductor (meissner effect) where as ac field can penetrate. Hence the diamagnetic nature of superconductor is a bulk effect and is not a surface effect, can only be confirmed only by ac susceptibility measurement. In the fully superconducting state, the sample is a perfect diamagnet and so $\chi' = -1$. Typically, the onset of a significant nonzero χ' is taken as the superconducting transition temperature [5].

So, it is concluded that ac susceptibility has many advantages over dc susceptibility. It is the reason of choosing ac susceptibility.

1.6 DIAGRAM OF TYPICAL AC SUSCEPTOMETER:

It consists of primary excitation field coil, a secondary pick up coil, a secondary compensation coil. An insulated copper wire is used for the winding of the coil. In the fig below, schematic diagram of a susceptometer designed by [ref] is shown. A four coil system is made which consist of two identical primary coil of 120 turns each and two secondary pick up coils of 600 turns each [6]. The coils are winded around a hollow cylinder of 1.2 cm in height. An ac magnetic field is generated by the 2 identical primary coils .An ac constant current source was coupled to an external oscillator which permits the measure of ac susceptibility over a broad range of discrete field amplitude, frequency temperature. And the pick up coils were winded beneath the field coils, with a shield of low temperature silk thread in tape was used to reduce their capacitive coupling to achieve a good thermal stability.

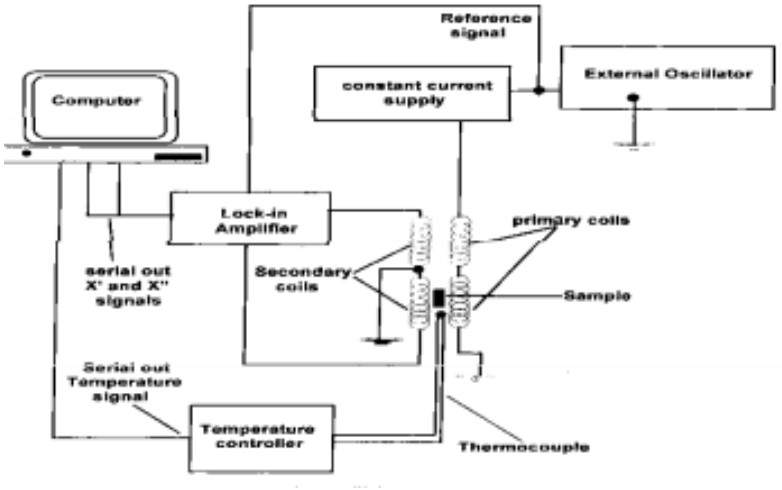

Fig 1.7 Diagram of an ac susceptometer [6]

The pick up and reference coils are connected here to the differential input of a computer controlled lock in amplifier.

Chapter-2

Design and fabrication:

2.1 Cross-Section view of 1st design:

Actually we have made our set up for two times. First time it was damaged at ~200^{0}C due to wrong material supplied. Then we made a second setup, whose data is shown here. In the following figure 2.1, the design of first set up is shown.

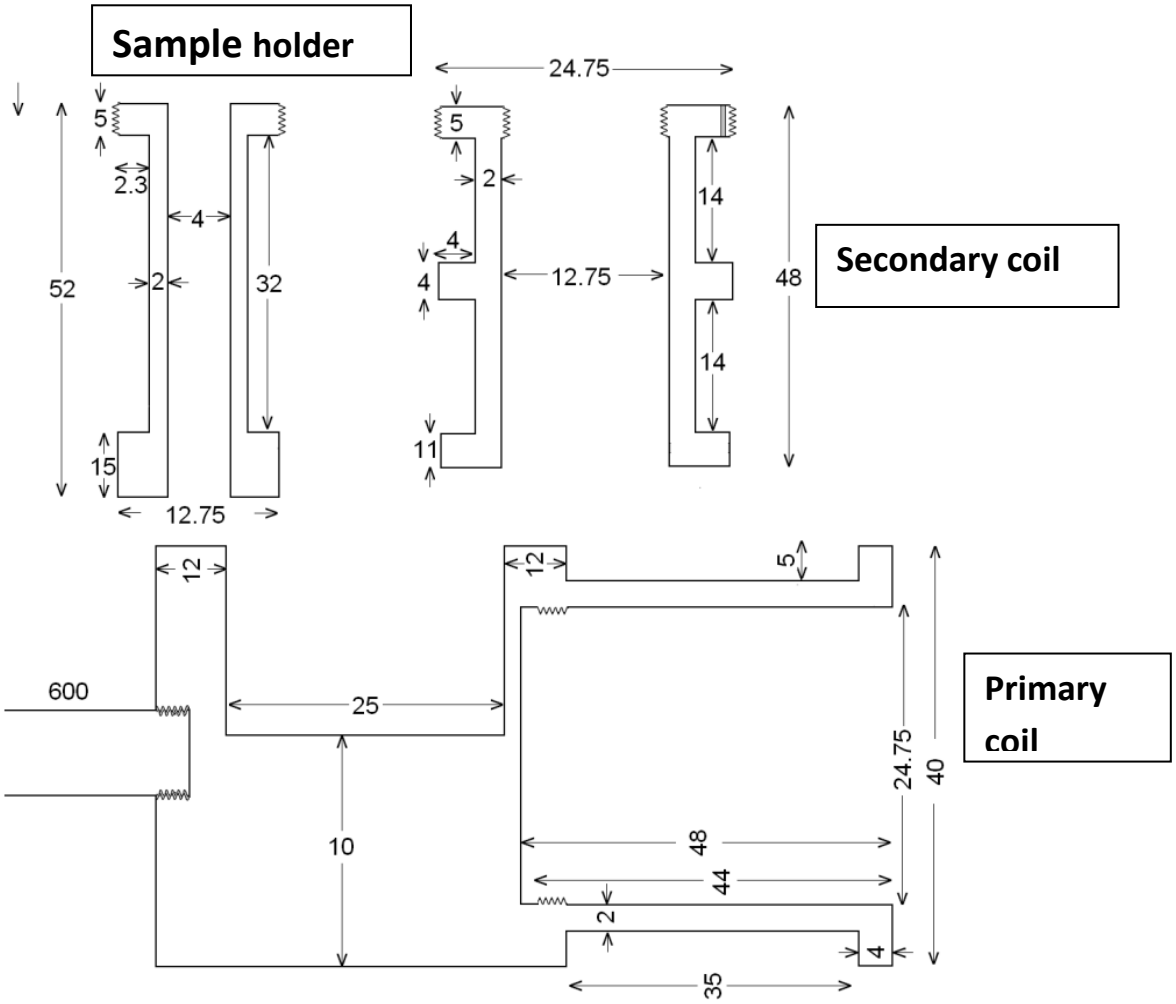

Fig 2.1 all parameters are in mm. Cross sectional schematic of the 1st design

Fig 2.2 Damaged picture of first set up

The primary and the secondary coils are winded with copper wire (150 micron). For the 1st design, the number of turns in primary coil is 1200 and in secondary coil it is 1000 in which 500 is clockwise and another 500 is anticlockwise. [7]. The number of winding layers in primary is 6 and in secondary is 7 in each. A quite simple design for the susceptometer is chosen as shown in the above figure. Indeed focus is put on the miniaturization of the device to achieve high sensitivity.

After the mishap of first set-up, a second set-up is designed. In the second design, the number of turns in primary and secondary both are 1000, with 500 clockwise and 500 anticlockwise in the secondary. The primary coil and two secondaries should be arranged properly [8]. This time we did not included a separate sample holder, rather we put our sample directly in one of the secondary. We can keep the secondary inside and primary outside and vice versa [9]. But in our project we kept the primary coil outside. Because when we put the secondary outside, comparably less induction occurs. So the former being positioned in between the later couple in order to allow modifications out the outer secondary for calibration.

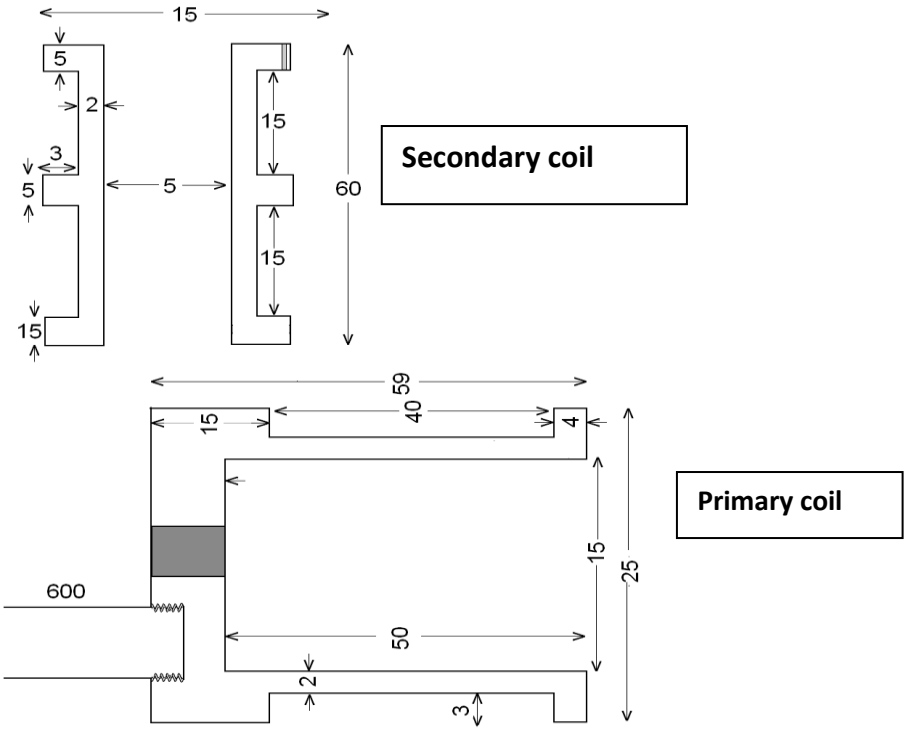

Fig 2.3 Cross section of second design

Fig 2.4 Picture of the second design

2.2 Magnetic field at the centre of the solenoid:

We have used the formula for the solenoid H= Ja F(α β)

Where

$$F(\alpha,\beta)=\frac{\mu\left(1+\sqrt{\alpha^2+\beta^2}\right)}{\left(\alpha+\sqrt{\alpha^2+\beta^2}\right)}$$

Here $\alpha = b/a$ and $= l/a$, where a and b are the inner and outer radius of the solenoid. $2l$ is the length of the solenoid.

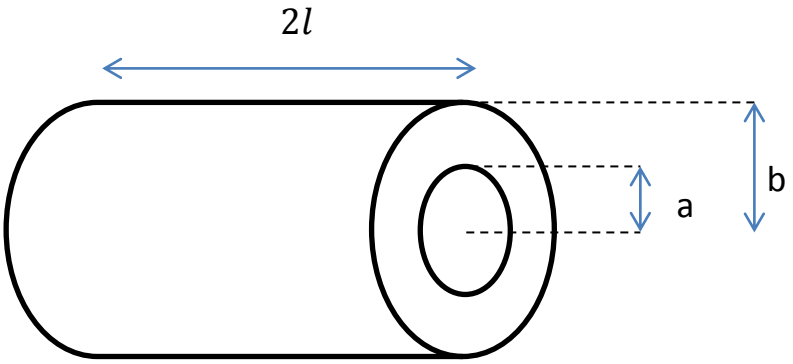

Fig 2.5 solenoid and its dimensions

Current density is J = I/A Where I= total current passing through the solenoid and A= total cross-sectional area offered to the current flow, $\{2l(b-a)\}$. In this method the change in flux dφ is measured as induced voltage V(t) in the secondary coil,

The measured rms voltage V across the two secondary coil is :-

$$V(t) = -d\emptyset/dt$$

The magnetic flux through the N turn oppositely wound coils of radius a is :-

$$\emptyset = \pi a^2 N M(t) \mu_0$$

With M(t) denoting the magnetic induction inside the sample averaged over the volume V.

So, $$V(t) = -\mu_0 \pi a^2 N dM(t)/dt$$

But for complex susceptibility χ_n' and χ_n'' one can do a Fourier expansion of $M(t)$

$$M(t) = \sum H_{ac} (\chi_n' \cos n\omega t + \chi_n'' \sin n\omega t)$$

Putting $M(t)$ in the eq of V(t) ,we get,

$$V(t) = V_0 \sum n(\chi_n' \sin n\omega t - \chi_n'' \cos n\omega t)$$

Where $V_0 = \mu_0 \pi a^2 \omega N H_{ac}$

The real and imaginary component of susceptibility χ_n' and χ_n'' are determined directly from $M(t)$ through the relationship

$$\chi_n' = \frac{1}{\pi H} \int_0^{2\pi} M(t) \sin(n\omega t) d(\omega t)$$

$$\chi_n'' = \frac{1}{\pi H} \int_0^{2\pi} M(t) \cos(n\omega t) d(\omega t)$$

Here H is alternating magnetic field(H_{ac}). n=1 denotes the fundamental susceptibility while n= 2,3,4… etc are the higher order harmonics associated with non linear terms in χ .

The magnetic field at the centre of the solenoid is given by :-

$$B = \mu_0 J a \, F(\alpha, \beta) \qquad (1)$$

where $F(\alpha,\beta)$ is the field factor which depends on the cross-sectional shape of solenoid.

$$F(\alpha, \beta) = \beta ln\{\frac{\alpha + (\alpha^2 + \beta^2)^{\frac{1}{2}}}{1 + (1 + \beta^2)^{1/2}}\}$$

where $\alpha = b/a$

$$\beta = l/a$$

For the set-up we have designed, the value of $a = 7.5mm$, $b = 12.5mm$ and $l = 20mm$

Putting these values we get , $\alpha = 1.67$ and $\beta = 1.33$ .So, the value of $F(\alpha,\beta)$ comes to

$$F(\alpha, \beta) = 0.59$$

The calculated amount of current passing through the solenoid is $I = 5\ \mu A$

So, the average current density $J = I/A$

$$A = 2l(b - a) = 200 * 10^{-6}$$

The value of J comes to $J = 0.25\ A/m^2$

So, $B = 13.89$ Tesla

$V_o = \mu_0 \pi a^2 \omega N H_{ac}$

$V_0 = 4\pi * 10^{-7} * \pi * (7.5 * 10^{-3})^2 * 2\pi * 843 * 1000 * 13.89$

$V_0 = 2.46 * 10^{-2}$ volts.

Every magnetic material has some demagnetization factor which depend on the shape. The actual susceptibility is

$$\chi_{ac} = \frac{\chi_m}{1\text{-}N\chi_m}$$

Here N is the demagnetization factor. Ref no[10]

2.3 Experimental set up at high temperature:

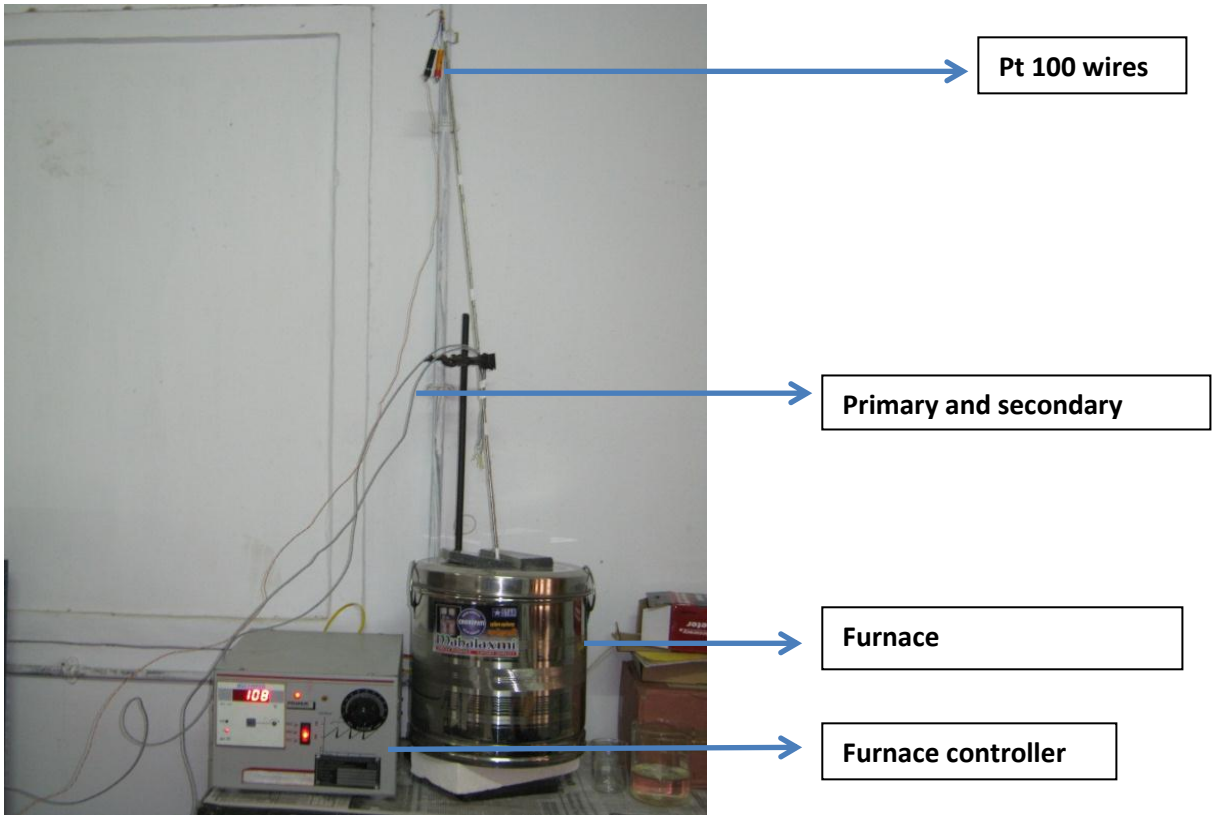

Fig 2.6 Experimental set up at high temperature

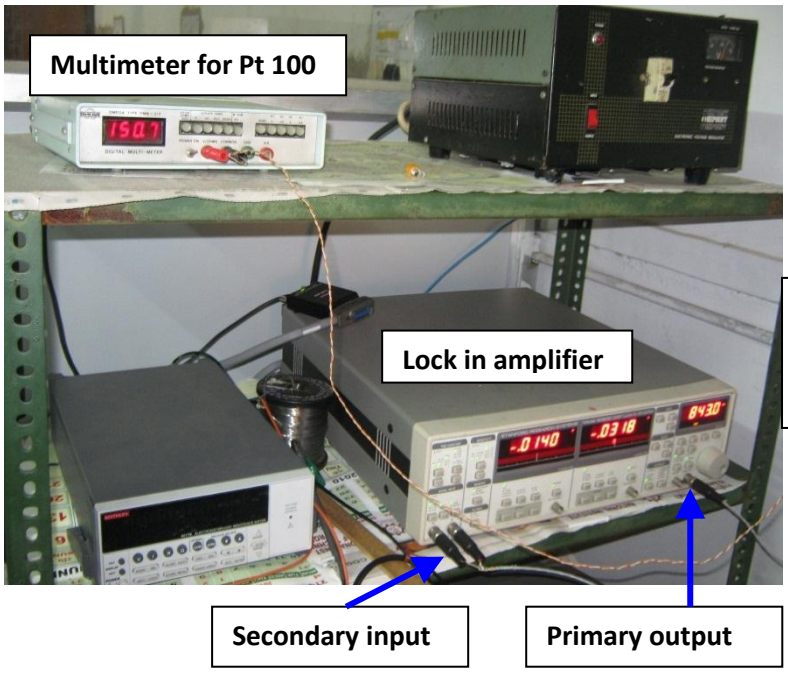

Fig2.7 Lock in amplifier at the time of high temperature measurement

2.4 The graphs of the susceptibility with sample and without sample.

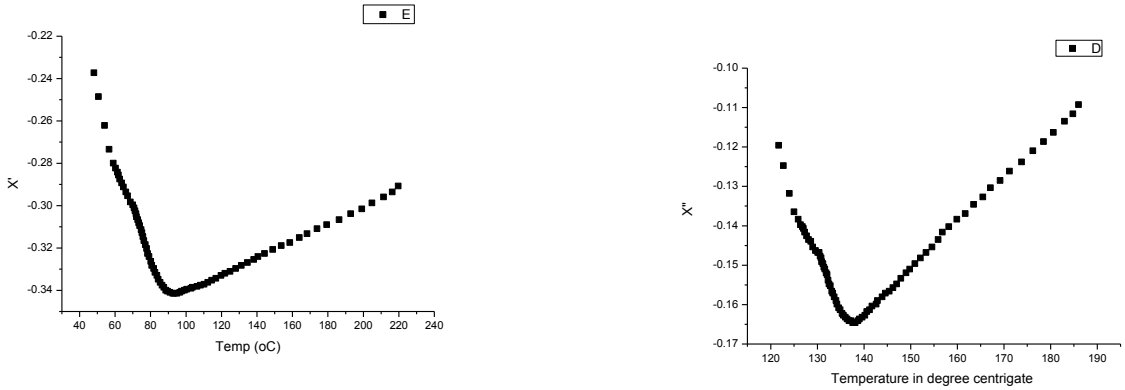

Fig 2.8 X' and χ" with sample

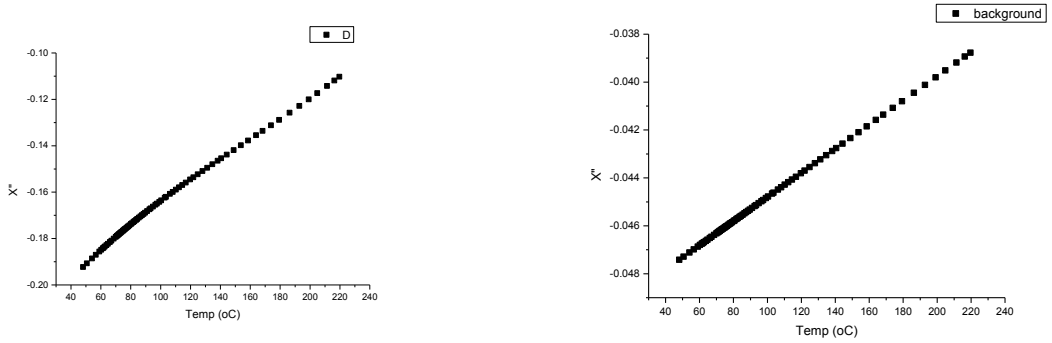

Fig 2.9 X' and χ" without sample

After subtracting susceptibility value without the sample from the susceptibility value without sample we get the actual result which will discuss in the result discussion part.

CHAPTER-3:

Sample Preparation

3.1 Sample selection:

Here in our project $La_{2/3}Sr_{1/3}MnO_3$ is chosen for sample under investigation. $La_{2/3}Sr_{1/3}MnO_3$ has been the subject of research for more than a decade for its immense applications in different fields as well as the interesting physics in it.

$La_{2/3}Sr_{1/3}MnO_3$ is the derivative of parent compound $LaMnO_3$. $LaMnO_3$ is an antiferromagnetic insulator and Sr doping at La site enhances ferromagnetic interactions in the compound. With increasing Sr content, the compound shows a variety of magnetic and electronic states (fig 3.1).

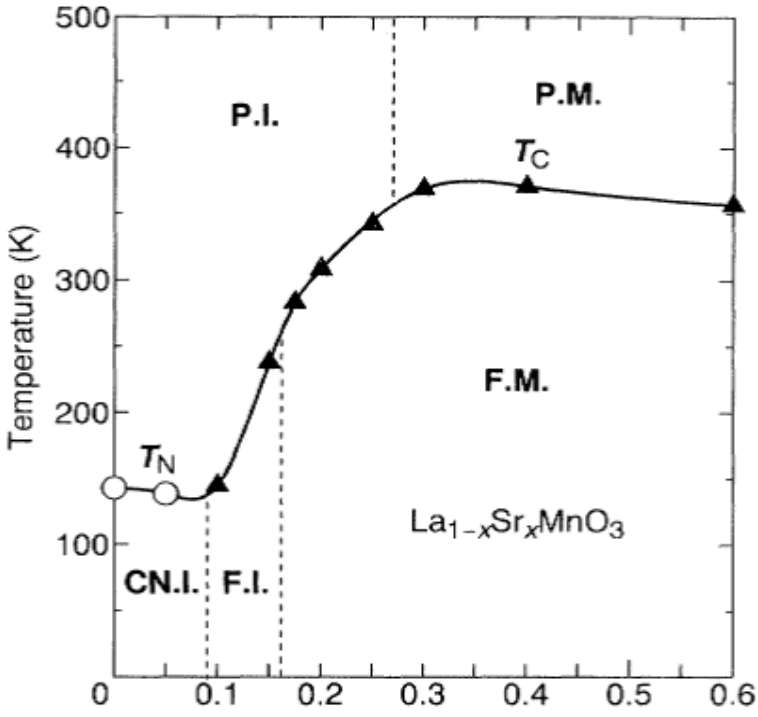

Fig 3.1 Magnetic Phase diagram of La-Sr-MnO3. Open circles and filled triangles are Neel temperature (TN) and curie temperature (Tc) respectively. The abbreviation mean paramagnetic Insulator (PI), Paramagnetic metal (PM), Spin canted insulator (CNI), Ferromagnetic insulator (FI) and ferromagnetic metal (FM) [11]

The structure of LaMnO3 is perovskite type orthorhombic structure. With increasing Sr content, the lattice parameter changes accompanying structural transformation from orthorhombic to rhombohedral. The tolerance factor which is a measure of microscopic distortion from the ideal perovskite structure (t=1) of the form ABO3 is defined as

$$t = \frac{R_A + R_O}{\sqrt{2}\left(R_B + R_O\right)}$$

where R_A, R_B and R_O are the ionic radius of A-site, B-site and oxygen ions respectively. For LSMO, the tolerance factor may be calculated using La^{3+} (0.136nm), Sr^{3+} (0.144nm), Mn^{3+} (0.0635nm), Mn^{4+}(0.0530nm) and O^{2-} (0.134nm) as,

$$t = \frac{R_{La^{3+}} + R_{Sr^{2+}} + R_{O^{2-}}}{\sqrt{2}\left(R_{Mn^{3+}} + R_{Mn^{4+}} + R_{O^{2-}}\right)} = 0.988$$

Value close to one indicates that perovskite structure for LSMO.

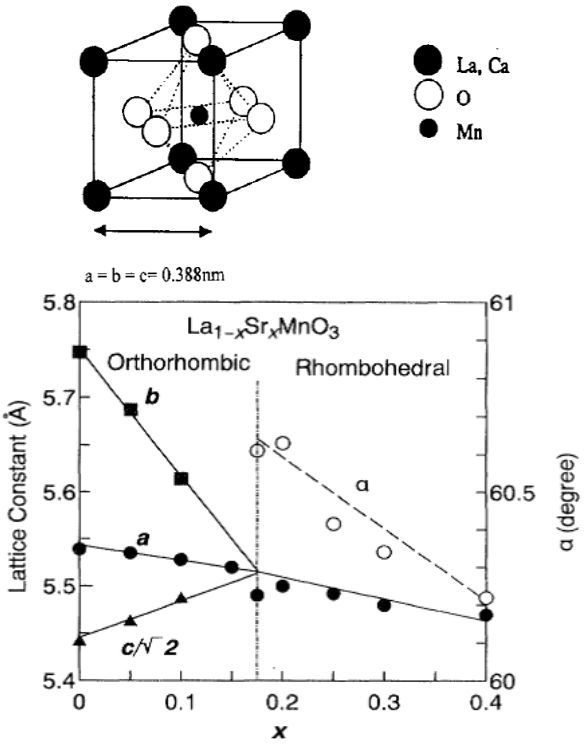

Fig 3.2 Perovskite structure and the lattice parameter of LSMO at room temperature graph Ref [17 &12]

The Sr doping in $LaMnO_3$ not only affects the magnetic and structural properties, but the electrical properties also undergo a profound change. The parent compound $LaMnO_3$ is an insulator and Sr doping brings metalicity in the compound. From the magnetic phase diagram and electrical conductivity data, it is evident that for Sr doping more than 20%, the sample becomes Ferromagnetic metal, with Curie temperature systematically shifting to higher temperatures. $La_{2/3}Sr_{1/3}MnO_3$ has ferromagnetic Curie temperature, Tc above room temperature, about 380 K and a large magnetic moment at room temperature (see fig 3.1, 3.3 & 3.4). Since its transition temperature Tc is also above room temperature, these materials find immense application in various fields.

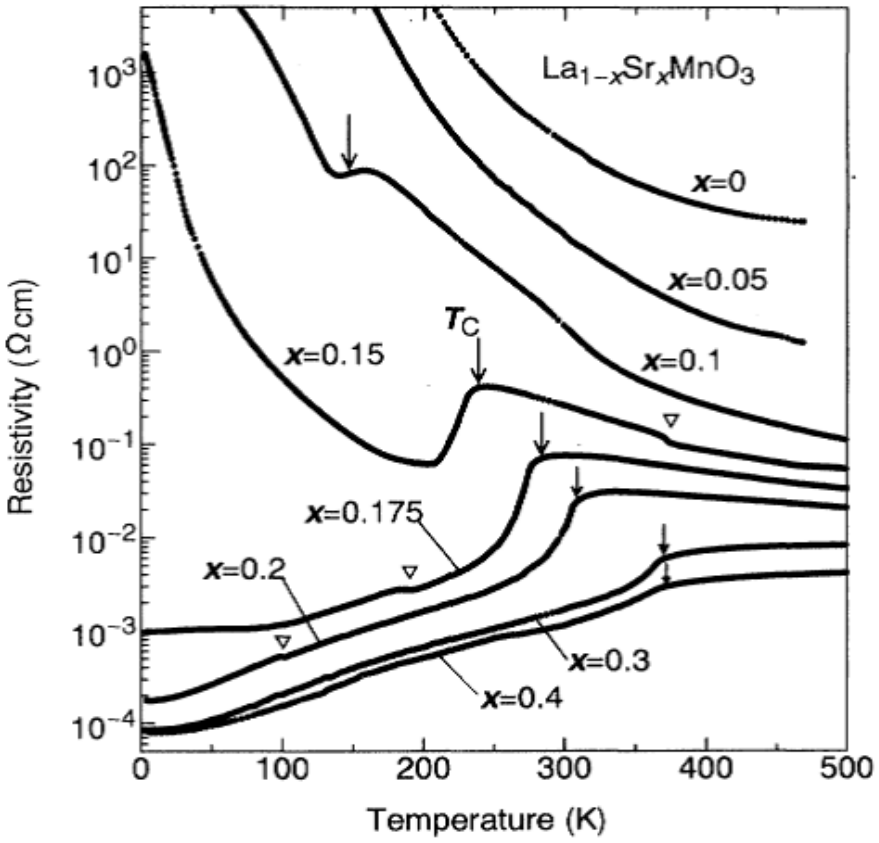

Fig 3.3 Temperature dependence of resistivity of LSMO. Arrows indicate the critical temperature of the ferromagnetic phase transition Ref no[12]

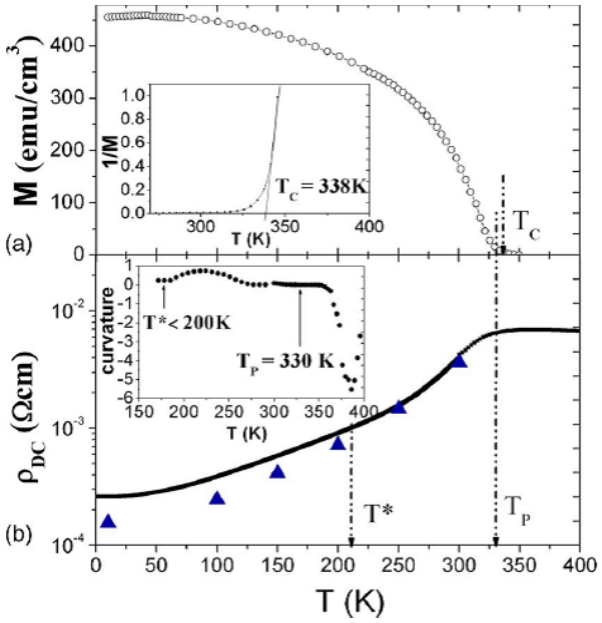

Fig 3.4 Temperature dependence of the Magnetization and resistivity of La2/3Sr1/3MnO3. Ref [13]

LSMO, especially $La_{2/3}Sr_{1/3}MnO_3$ & $La_{0.7}Sr_{0.3}MnO_3$. Belong to special class of metals known for its half metallic behaviour. Half-metallic materials are characterized by the metallic behaviour due to electrons of same spin. From the following figure, which plots density of states (DOS) as a function of energy, it can be seen that Fermi level is surrounded only by spin-up electrons. DOS for spin-down electrons is zero at the Fermi level. Hence the conduction process, which is due to electrons near the Fermi level, is governed only by one type of spin orientated electrons. Half-metallic ferromagnet having 100% spin polarization (e.g., $La_{0.7}Sr_{0.3}MnO_3$) offers potential technological applications such as a single-spin electron source, and high-efficiency magnetic sensors.

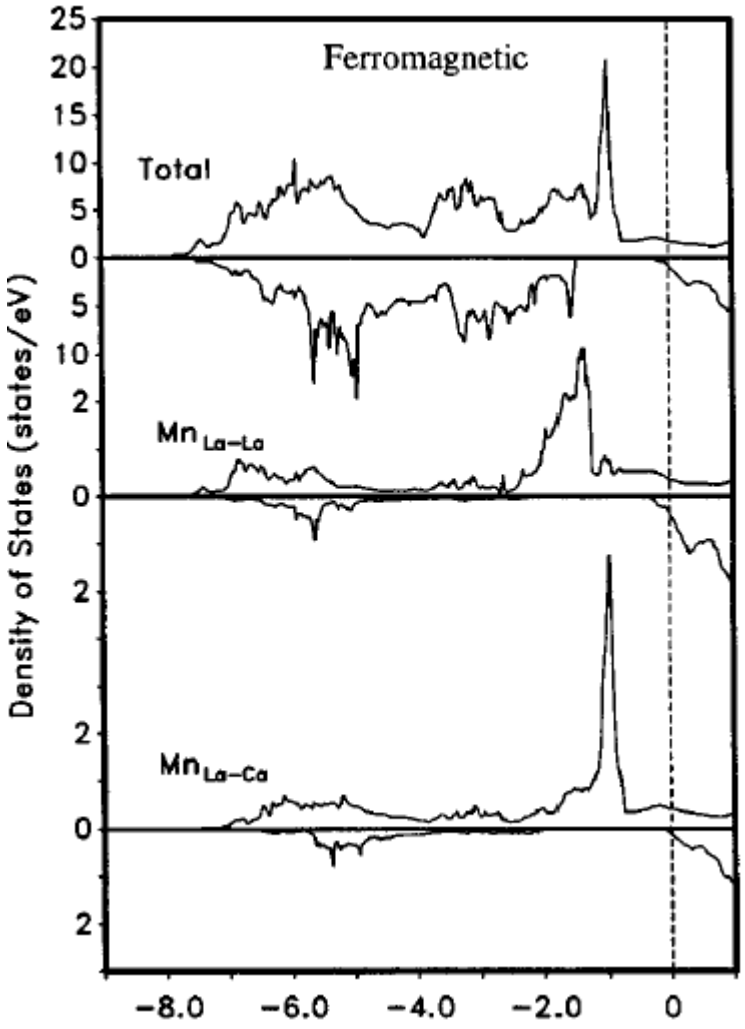

Fig 3.5 The total DOS and local DOS on each equivalent Mn ion for the x=1/3 in $La_{1-x}Sr_xMnO_3$ for the Ferromagnetic ordering. It can be seen that at Fermi level (dotted line), only up spin DOS is present and down spin DOS is absent. Hence the conductivity process is only due to up spin electrons [12] .

Thin films of LSMO finds tremendos applications in GMR (Giant Magneto Resistance) or TMR (Tunneling Magneto Resistance) devices, organic thin-film spin valves, photoconductivity, magnetic field sensors, etc. Recently, a FET (Field Effect Transistor) has been made from $BiFeO_3$ as the dielectric and ferromagnetic $La_{0.7}Sr_{0.3}MnO_3$ as the conducting channel. The researchers claim that two distinct exchange-bias states can be reversibly switched by switching the ferroelectric polarization of $BiFeO_3$. This may enable a new class of electrically controllable spintronic devices based on controllable spin-polarized currents.

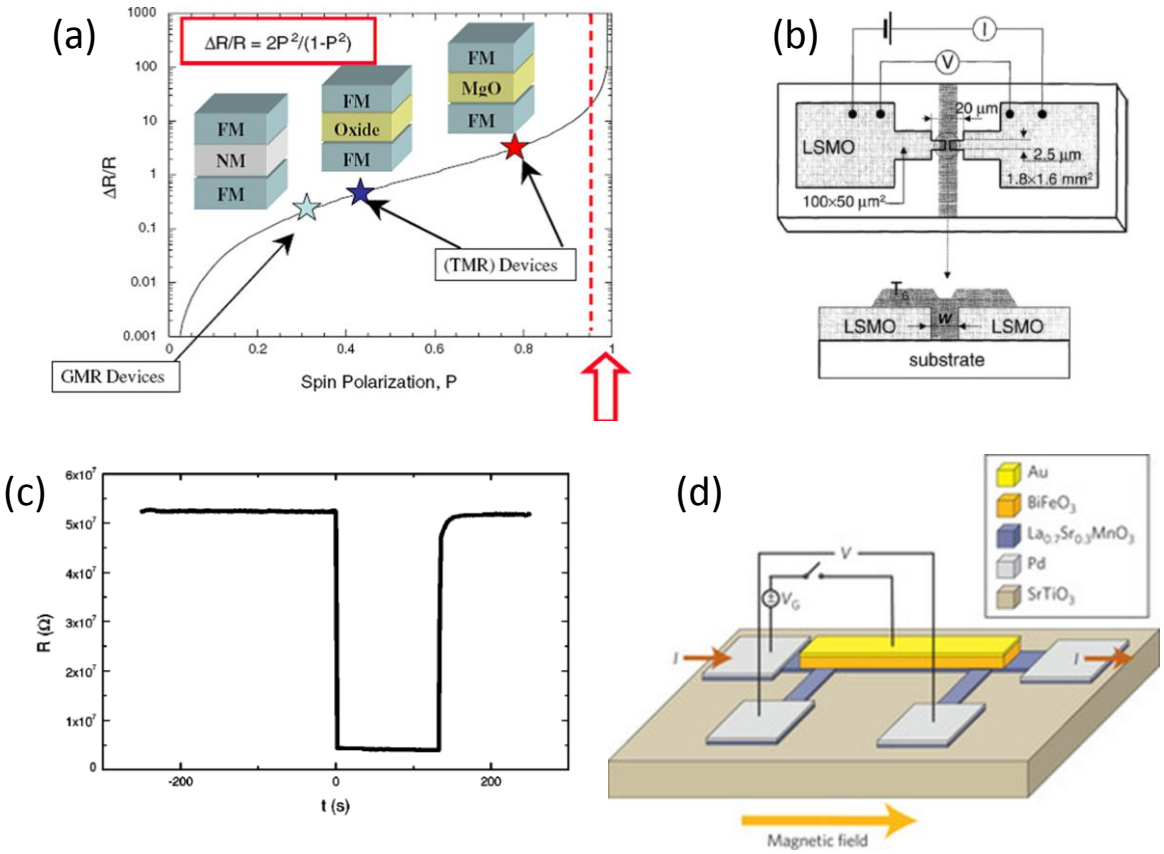

Fig no 3.6

(a) Tunnelling Magneto resistance junction [14]

(b) Schematic top view and cross section of a hybrid LSMO/T6 (sexithienyl)/LSMO junction based organic thin film valve. [15]

(c) Photoconductivity in LSMO. At t =0, light switched on and at t =130s light switched off [16]

(d) A schematic of the BFO/LSMO field-effect device [18].

Recently magnetic nanoparticles systems have initiated great interest because of their tunable physical properties and their applications in technological fields such as magnetic recording media, magnetic sensors, permanent magnets, Ferro fluids, magneto caloric refrigeration, magnetic resonance imaging (MRI) enhancement, magnetically guided drug delivery etc**.** The

magnetic properties of nanoparticles changes on changing the size and shape of particles, particle size distribution, finite-size effect and dipole dipole interaction. Recently $La_{0.67}Sr_{0.33}MnO_3$ nanoparticles have been found suitable for hyperthermia treatment. Magneto caloric is another area for which LSMO has been investigated. In the fig 3.7, entropy change due to magnetic field is plotted as a function of temperature for three materials namely, La-Ca-MnO, La-Ba-MnO, La-Sr-MnO. Entropy change is the measurement magnetocaloric efficiency. It can be seen that, for a hot country like India [where room temperature reaches upto 325K], LSMO is more suitable for magnetocaloric applications.

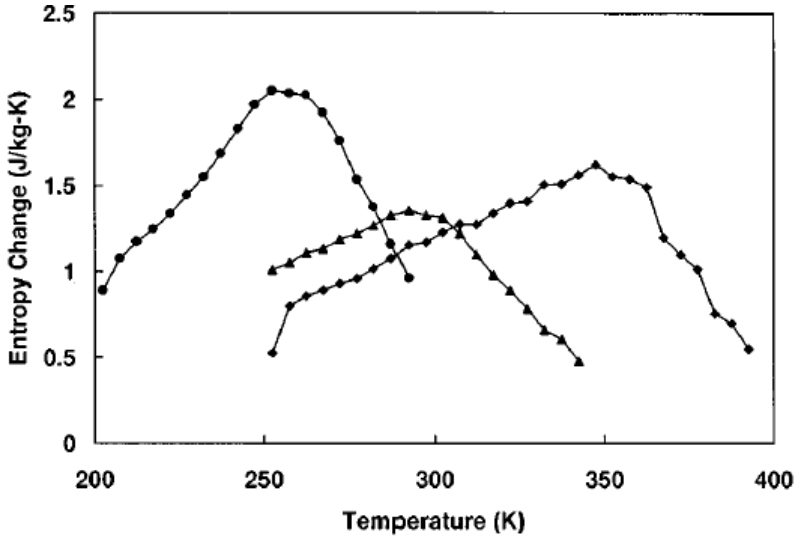

Fig 3.7 Entropy change for a field change of 5T of La-Ca-MnO, La-Ba-MnO ,La-Sr-MnO. [19]

3.2 Different techniques involved in Preparation:

The citrate-gel route:

The precursors are taken in the form of acetates. The metal acetates are dissolved in water. Then the solution was mixed with citric acid, in which ratio is 1:1. The solution is then heated to 80 °C for 2 hours so that it becomes gel. The gel is further heated to 400^0C to form foam like powder. The foamy precursor decomposed to give very light, homogenous, black-colour flakes of extremely fine particle size. [20]

Sol gel combustion method:

In this method the precursors in the form of nitrates, are dissolved in waters. To this solution, some fuel is added to initiate combustion. This method is described below in detail, as we have followed this method.[21]

Spray drier method

An aqueous solution of lanthanum, strontium and manganese nitrates was mixed from starting solution in the desired stoichiometric ratios. This solution was spray-dried in a spray drier. Spray dryer converts liquid feed into a uniform powder in a continuous operation. Spray drying starts with atomization of product into a spray of fine droplets as it is fed into the drying (120^0C) chamber. The fine droplets sprayed into the chamber become suspended in heated gas stream. Then droplets are evaporated and dried to spherical powder. Dried powder is separated from the gas stream and connected in the base of the drying cyclone chamber [21]

LSMO preparation by sol gel capped with Au:

Sometimes, the nano-particles need to be capped by bio-compatible material for its application in drug delivery. Here the LSMO nanoparticles were prepared by a sol-gel procedure using Diethylene-triamine-penta-acetic acid and $Mn(CH_3COO)_2,H_2O$ in the required stoichiometric ratio were used as precursors. $Au(OOCCH_3)_3$ is used for gold caping agent [22].

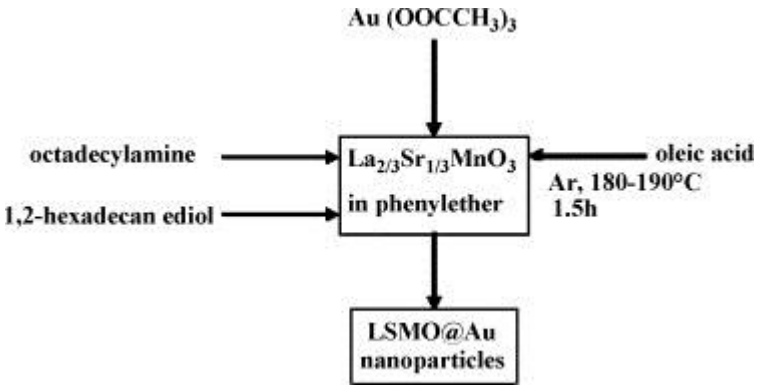

Fig 3.8. Synthesis scheme of LSMO nanoparticles coated with Au [22]

3.3. LSMO PREPARATION:

Here we report on the preparation of nanoparticles $La_{0.67}Sr_{0.33}MnO_3$. Phase formation, crystal structure and particle size were studied by X-ray diffraction (XRD).

Nanoparticles of LSMO are prepared by auto combustion sol-gel method. The precursors chosen for the synthesis are $La(NO_3)_3.6H_20$, $Sr(NO_3)$ and $MnCO_3$. Stoichiometric amounts are taken as 0.67% of 0.02mole, 0.33% of 0.02mole, 0.02 mole respectively. Glycine was taken as a combustion agent. It is notified that the ratio of glycine: metal nitrate is 1:1.

The reactants were dissolved into the distilled water and stirred for 30 minutes continuously. The solution is now colourless. Then glycine is added into the solution. The solution was then heated with constant stirring at 80 °C to evaporate the excess solvent. After 3 hours of heating the solution converted to a viscous gel. Then after burning due to glycine agent the gel is converted to the black powder. The gel was dried at 250 °C. After collecting the powder, calcination is done at 600 °C for 2 hours. The furnace heating rate is maintained 4^0C/minute. After cooling the sample is collected from the furnace and is grinded in a agate-motor. The grinded powder is now ready for necessary characterization. And after calcination sintering has done at 825^0c for 5 hours. The sample is pressed into the pellet.

Then the characterization is done. By XRD Phase formation and crystal structure of the powders were checked by using Cu Kα radiation source in the 2θ scan range from 20° to 80^0c. From the X-ray peak width the average particle sizes of the samples were estimated by using the William Hall method. The pellet is cut into a small piece of rectangular shape and wrap in a Teflon tape to use in ac susceptometer in high temperature. Finally the ac susceptibility was measured by the susceptometer which was fabricated already.

3.4 Flow chart to prepare LSMO:

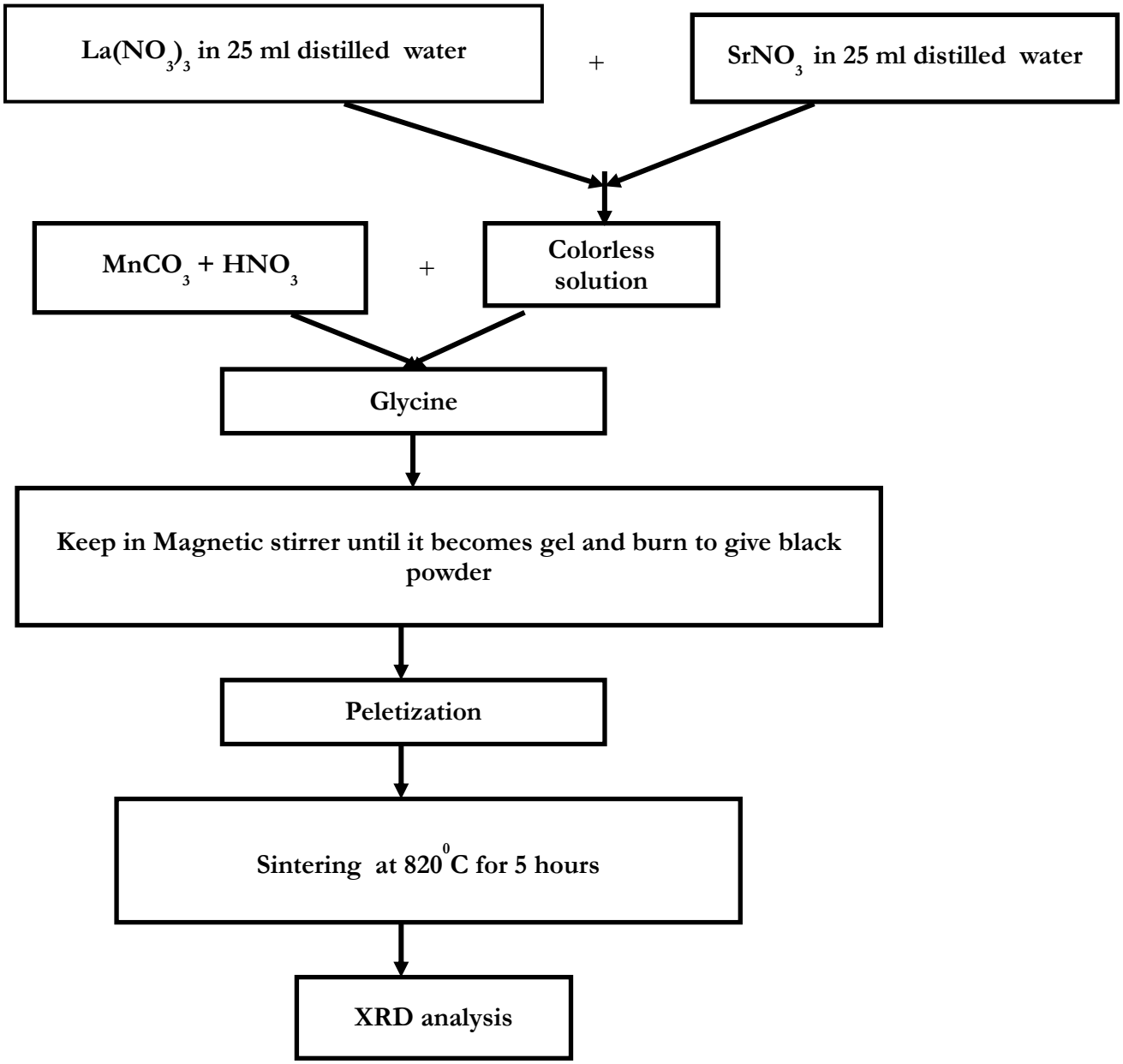

Chapter-4

RESULT AND DISCUSSION

4.1. XRD analysis of the LSMO:

The sintered sample is first analysed for its phase formation via x-ray difraction (xrd) analysis. The xrd plot of LSMO sample is shown in fig 4.1. The xrd data is taken in the 2θ range of 20^0 to 60^0. In this range, five prominent peaks are observed. All peaks could be indexed to the respective (hkl) planes of LSMO (PDF #401100) having lattice parameters a =5.484Å, b= 5.534 Å and c= 7.791 Å, space group P2/c (13). No extra peaks were found, indicating that the sample is single phase.

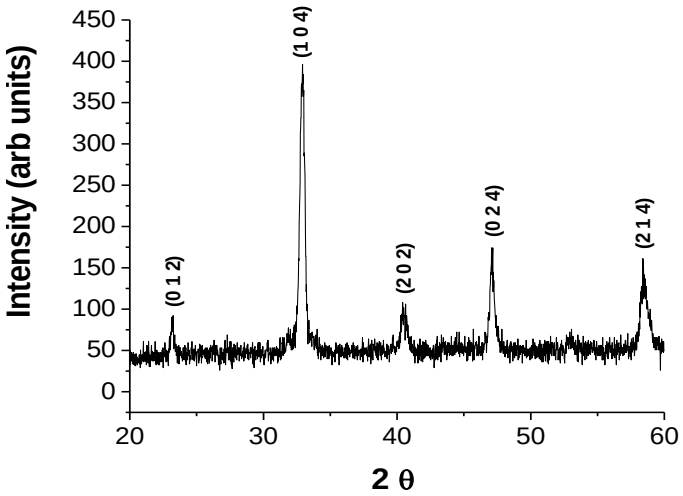

Fig. 4.1 XRD analysis of LSMO

From the XRD data, FWHM and 2Θ for all the five peaks were noted down and analysed using Williamson Hall method,

$\beta \cos\theta = 4\xi \sin\theta + \lambda/d$

Where d= crystallite size, λ= Wavelength of x-ray, ξ= strain, β= FWHM

A graph is plotted between β Cosθ and 4 Sinθ, for all the five peaks. The plot is than fitted for straight line fitting so that the slope gives strain (ξ) and the intercept is λ/d

From the graph we have

λ/d= intercept = 0.00189

Using $\lambda = 1.54A^0$, we have d = 81.50 nm and slope = 0.00428

So the crystallite size is 81.5 nm and the strain is $\xi = 0.00428$

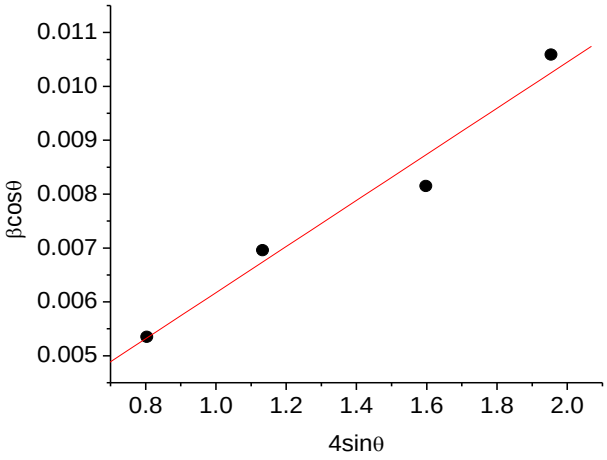

2Θ	FWHM
23.18727	0.24876
32.91059	0.34508
40.52436	0.47401
47.10922	0.30392
58.50651	0.56196

Fig 4.2 Plotting of XRD peak using Williamson Hall method.

4.2. Ac Susceptibility of the LSMO:

The sintered sample was cut into cylindrical shape weighing 0.014 gm. The rectangular shaped sample was wrapped with Teflon tape and carefully placed at the centre of one of the coils of secondary coil. Sufficient care is taken in placing the sample in the middle of the coil in order to avoid the edge effect. The whole set up is placed inside the furnace for high temperature susceptibility measurement.

First the setup is heated till 185^0C and we cool the system gradually up to room temperature. Readings were taken at the time of temperature rising as well as cooling. The x-component (in-phase) and the y-component (out-of-phase) component of the signal are recorded as a function of temperature. These x and y component is then converted in volume susceptibility

by dividing with parameter v_0. The variation of in-phase(χ') and out-of-phase(χ") susceptibilities with temperature is shown in Fig 4.3. As the sample is cooled down from high temperature, the susceptibility is almost constant having very low value. Around 90^0C, the susceptibility starts rising sharply and till the lowest temperature of measurement, no saturation is observed. The sharp rise at 90^0C in susceptibility indicates ferromagnetic ordering below this temperature. The rise in susceptibility is similar for both in-phase and out-of-phase components of susceptibility. This reflects ferromagnetic nature of LSMO, as per literature. For comparison, the susceptibility data is compared with ref. [23] (fig 4.4). The ref data scale is in Kelvin where as our data scale is degree centigrade. In Kelvin scale, 90^0C corresponds to 363K. It may be seen that our data is in good agreements with that in ref [23]

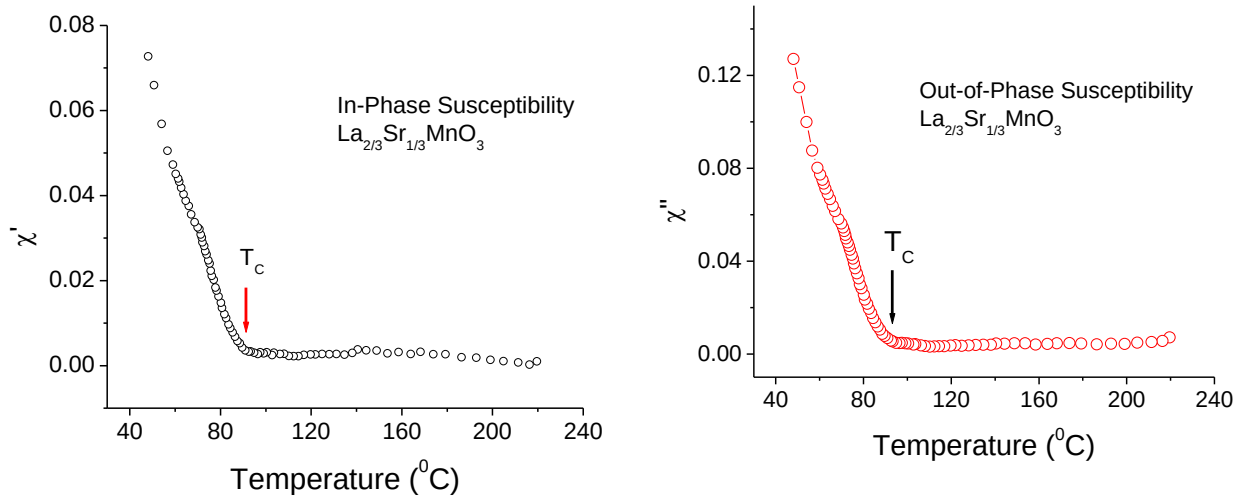

Fig.4.3 The in phase and out of phase susceptibility vs temperature at high temp measurement.

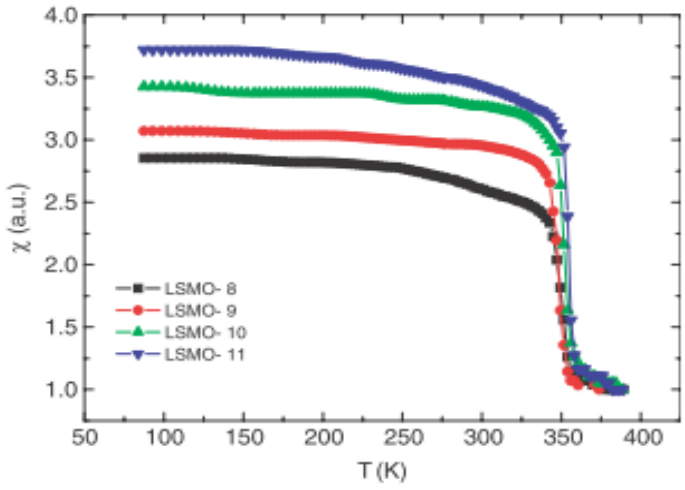

Fig. 4.4 The standard graph of

4.3 Conclusion:

We have made the susceptometer for two times.1st times when it was made it consist three parts.one is sample holder, one is primary coil and another one is secondary coil. After designing the setup we prepared the LSMO for the susceptibility measurement. In the time of high temperature measurement at 200^{0}c it burned and it get totally damaged. It got damaged due to wrong material. We have chosen Teflon material to make the set up. Teflon has the melting point 600^{0}c.So it should not damage. But the material which we bought 1st time was poor quality. 2nd time we bought good quality material and again designed it. But in this time some modification has done. This time we neglect the sample holder part because of making good contact of sample with the magnetic field.

In the time of damaging of the 1st set up the sample was also damaged. So we have to prepare this again. After preparing the pallet it cut into a rectangular shape and insert it inside the secondary coil.

The XRD peak for LSMO matches accurately with the standard value. After getting the Susceptibility value when we plot it with temperature we get the transition of LSMO in accurate position (364k) .

So my set up is working properly and the sample which I have made is also properly made.

Chapter 5

Appendix

XRD Analysis of $CoFe_2O_4$:

Actually this is a combined project of me and Rakhee Sharma. We have prepared CFO also.

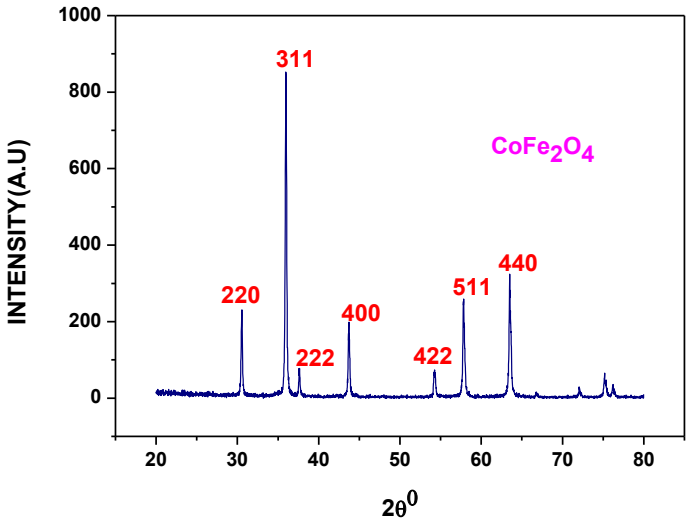

41

Fig 5.1 XRD analysis of CFO

But the details you will get in her thesis. The structural characterization of the sample was carried out by XRD technique. The above graph is in good agreement with the standard one. So, it was confirmed that the sample was prepared properly.The crystallite size is calculated using the Scherrer formula.After preparing the CFO we insert it Inside the secondary for susceptibility measurement.

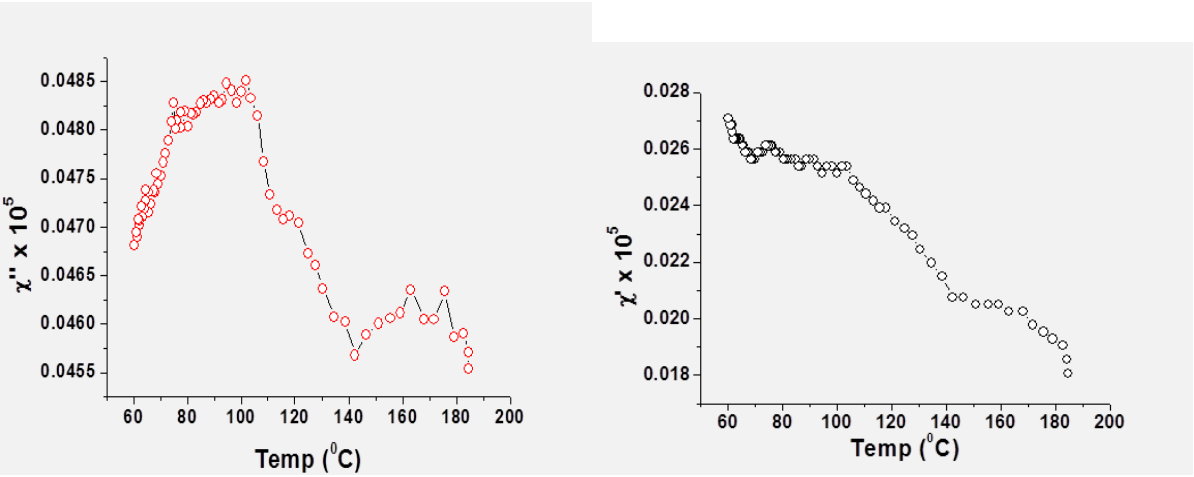

Fig5.2 χ '' part and the χ' part with the température at the time of high température measurement

As the transition temperature for CFO is high about 700k so the transition to paramagnet is not clear at 473k.

References

1. Charles Kittel *introduction to solid state physics* Johns Wiley & sons 1995

2. B. D. Cullity & C D Graham, *Introduction to magnetic material* 2nd edition, Wiley, 2009

3.Rev.sci.Instrum,**30**,548 1959

4. Joel.s Miller,Mare Drillon Wiley-Vch 2002

5. Robert A Hein,Thomas L Francavilla,D H Liebenberg, *Magnetic Susceptibility of Superconductors & other spin system springer*(1991)

6. M I Youssif,A. A. Bahgat* and I.A Ali , *Egypt. J. Sol*, **23**, 231 (2000)

7. 18. Martin Nikolo Am . *j physics A guide to ac current susceptibility* **63** 1995

8. 19. T. Heitmann,1, J. Gaddy,1,2 J. Lamsal,1,2 M. Petrovic,2 and W. Montfrooij *journal of applied physics* **107**, 09E143 _2010

9. 20. L. E. Floresa) and C. Noda C. Abascal J. L. Gonza´ lez **69**, NUMBER 10

10. 21. H. Kunkel, FL M. Roshko, W. Ruan, and G. Williams J. Appl. Phys. **69** (8), 15 April 1991

11. A. Urisibara, Y. Moritomo, T. Arima, A.Asamitsu, G Kido, Y.Tokura *insulator metal transition* **51** No 20

12. D M Edwards Dept. of Mathematics, *Ferromagnetism and electron phonon coupling in Magnetites* 2008

13. A. M. Haghiri-Gosnet,1,M. Koubaa,2 A. F. Santander-Syro,3,4 R. P. S. M. Lobo,3 Ph. Lecoeur,1 and B. Mercey *physical review* B **78**, 115118 _2008_

14. B Nadgorny J. Phys.: Condens. Matter **19** (2007) 315209 15pp iop publishing

15. S. M. Wu, Shane A. Cybart, P. Yu, M. D. Rossell, J. X. Zhang, R. Ramesh & R. C. Dynes, *Nature Materials*, 9,756–761(2010)

16. R. Cauro,1 A. Gilabert,2 J. P. Contour,3 R. Lyonnet,3 M.-G. Medici,2 J.-C. Grenet,1 C. Leighton,4 and Ivan K. Schuller4 PHYSICAL REVIEW B, **63**, 174423 *American Physical Society* 2001

17. W J M Naber, S Faez and W G van derWiel J. Phys. D: Appl. Phys. **40** (2007) R205–R228 *journal of physics*,I O P publishing

18. S M Wu,Shane,A Cybart,P Yu *Natural materials* **9** 756 [2010]

19. Andrew M. Mance, Joseph V. Mantese, and Adolph L. Micheli Magnetocaloric properties of doped lanthanum manganite films J. *Appl. Phys*. **79** (1), 1 January 1996

20.V Ravi, S D Culkarni, V Samuel,J Mona *Ceramic International* **33**, 1129[2007]

21.D Grossin ,J G Noudem *Solid state science* **6**, 939 [2004]

22.O Pana,R Turcu, M L Soran ,C Leostean *synthetic metal* **160** 1692 [2010]

23. G. Venkataiah and P. Venugopal Reddy Phase Transitions **82,** No.2, February 2009, 156–166

24. Puri & Babbar *Solid state Physics* 1996

25. J.M.D Coey, M Viret, *mixed valance magnetites* **48** No 2 167-293 p

Fig 5.1 XRD analysis of CFO